Available online at www.sciencedirect.com
ScienceDirect
Journal of Biotechnology 132 (2007) 375–384
Journal of BIOTECHNOLOGY
www.elsevier.com/locate/jbiotec

Response of fluxome and metabolome to temperature-induced recombinant protein synthesis in *Escherichia coli*

Christoph Wittmann [a,*], Jan Weber [b], Eriola Betiku [b], Jens Krömer [a], Daniela Böhm [b], Ursula Rinas [b]

[a] *Biochemical Engineering, Saarland University, Saarbrücken, Germany*
[b] *Biochemical Engineering, German Research Center for Biotechnology (now renamed in Helmholtz Center for Infection Research), Braunschweig, Germany*

Received 19 March 2007; received in revised form 7 June 2007; accepted 3 July 2007

Abstract

The response of the central carbon metabolism of *Escherichia coli* to temperature-induced recombinant production of human fibroblast growth factor was studied on the level of metabolic fluxes and intracellular metabolite levels. During production, *E. coli* TG1:pλFGFB, carrying a plasmid encoded gene for the recombinant product, revealed stress related characteristics such as decreased growth rate and biomass yield and enhanced by-product excretion (acetate, pyruvate, lactate). With the onset of production, the adenylate energy charge dropped from 0.85 to 0.60, indicating the occurrence of a severe energy limitation. This triggered an increase of the glycolytic flux which, however, was not sufficient to compensate for the increased ATP demand. The activation of the glycolytic flux was also indicated by the readjustment of glycolytic pool sizes leading to an increased driving force for the reaction catalyzed by phosphofructokinase. Moreover, fluxes through the TCA cycle, into the pentose phosphate pathway and into anabolic pathways decreased significantly. The strong increase of flux into overflow pathways, especially towards acetate was most likely caused by a flux redirection from pyruvate dehydrogenase to pyruvate oxidase. The glyoxylate shunt, not active during growth, was the dominating anaplerotic pathway during production. Together with pyruvate oxidase and acetyl CoA synthase this pathway could function as a metabolic by-pass to overcome the limitation in the junction between glycolysis and TCA cycle and partly recycle the acetate formed back into the metabolism.

Keywords: Human basic fibroblast growth factor; Adenylate energy charge; Cellular stress; ^{13}C metabolic flux

1. Introduction

Escherichia coli is one of the key microorganisms applied as heterologous host for the production of recombinant proteins due to its relative simplicity, its inexpensive and fast high density cultivation, the well known genetics and the large number of compatible molecular tools available (Sorensen and Mortensen, 2005). Hereby the expression of the target protein is usually induced at a certain time point of the cultivation, whereby temperature shift and the addition of an inducer molecule are the most frequently used approaches. A remaining bottleneck, however, is related to cellular stress, which is typically associated with the overexpression of heterologous genes, i.e. recombinant protein production (Wegrzyn and Wegrzyn, 2002). The resulting metabolic burden displays a critical factor with respect to quantity and quality of protein production so that many attempts have been made to improve the production by overcoming the stress response (Hoffmann and Rinas, 2004). A novel strategy that becomes available today and seems also promising to be applied to recombinant protein production by *E. coli*, is targeted metabolic engineering of the central metabolic pathways (Balbas, 2001). These pathways play a crucial role since they supply energy, reduction equivalents and precursor molecules for the recombinant product and the cell's housekeeping needs. In the field of recombinant protein production, however, only very few successful metabolic engineering examples are reported (De Anda et al., 2006; Kim and Cha, 2003; Picon et al., 2005). This is to a large extent due to the fact that

* Corresponding author at: Biochemical Engineering, Saarland University, POB 151150, 66123 Saarbrücken, Germany. Tel.: +49 681 302 2205; fax: +49 681 302 4572.
E-mail address: c.wittmann@mx.uni-saarland.de (C. Wittmann).

0168-1656/$ – see front matter © 2007 Elsevier B.V. All rights reserved.
doi:10.1016/j.jbiotec.2007.07.495

metabolic engineering prerequisites a detailed knowledge of the underlying metabolic network for the identification of promising targets and that today the exact response of fluxes and metabolites upon protein production are only poorly understood. In this regard the present work investigates the metabolic response of the central metabolic pathways in *E. coli* to temperature-induced production of human basic fibroblast growth factor (hFGF-2), a non-disulfide-bonded small protein. The study includes comparative analysis of metabolic carbon fluxes, i.e. the fluxome, and of intracellular metabolite levels, i.e. the metabolome, in control and producing cells of *E. coli*.

2. Material and methods

2.1. Strains, plasmids and medium

Escherichia coli TG1 supE hsdΔ5 thi Δ(lac-proAB) F'[traD36 proAB$^+$ lacI^q lacZΔM15] (Carter et al., 1985) was used as host to produce human basic fibroblast growth factor (hFGF-2). The heterologous hFGF-2 gene was encoded on the plasmid pλFGFB, which had been derived previously from the expression vector pCYTEXP1 (Seeger et al., 1995). Recombinant gene expression was controlled by the $\lambda P_R P_L$ tandem promoter/thermolabile repressor cI857 system and induced by temperature shift from 30 to 42 °C. *E. coli* TG1:pCYTEXP1, carrying the expression vector without structural gene, served as control. The used minimal medium contained (per liter) 15 g glucose in bioreactor cultures or 10 g glucose in shake flask cultures, 8 g $(NH_4)_2SO_4$, 0.8 g $(NH_4)_2HPO_4$, 2.7 g KH_2PO_4, 1 g $MgSO_4 \cdot 7H_2O$, 12 mg Fe(III)citrate, 0.5 mg $CoCl_2 \cdot 6H_2O$, 3 mg $MnCl_2 \cdot 4H_2O$, 0.3 mg $CuCl_2 \cdot 2H_2O$, 0.6 mg H_3BO_3, 0.5 mg $Na_2MoO_4 \cdot 2H_2O$, 1.6 mg $Zn(CH_3COOH)_2 \cdot 2H_2O$, 350 mg citric acid$\cdot H_2O$, 1.7 mg EDTA, 4 mg thiamine, and 40 mg ampicillin. For metabolic flux analysis the naturally labeled glucose was replaced by 99% [1-^{13}C] glucose (Campro Scientific, Veenendaal, The Netherlands).

2.2. Cultivation conditions

Comparative growth experiments at 30 °C and at 42 °C were carried out in 1000 mL baffled shake flasks with 200 mL medium. Cultures were inoculated to an initial optical density of 0.1 with an overnight grown pre-culture. For metabolic flux analysis cultivation was performed in 100 mL shake flasks with 15 mL medium. To assess the fluxes during growth, cultures were inoculated with an overnight pre-culture to an initial optical density OD_{600} of about 0.05 and grown at 30 °C for 6 h to an optical density between 1.1 and 1.2 for before cell harvest. For flux analysis during production at 42 °C, cells pre-grown at 30 °C on unlabeled glucose to an optical density of 0.5 were collected by centrifugation, resuspended in tracer medium containing labeled glucose and incubated for 4 h at 42 °C up to an optical density of about 2.8 (for *E. coli* TG1:pCYTEXP1) and 2.0 (for *E. coli* TG1:pλFGFB) prior to cell harvest. For metabolome analysis, cultivation in a 2 L bioreactor (Type SGI 7F-Set2, Setric Genie Industriel, Toulouse/France) was carried out at 30 °C, pH 6.6 and a stirring speed of 800 rpm. A constant aeration rate of 1.33 vvm was achieved by a mass flow controller (Brooks, Netherlands).

2.3. Substrate and product analysis

Cell concentration was determined via quantification of optical density (OD_{600}) or cell dry mass (Korz et al., 1995). The concentration of hFGF-2 was determined by SDS-PAGE analysis as reported (Seeger et al., 1995). Glucose and organic acids, i.e. acetate, lactate, pyruvate, and succinate, were analyzed by HPLC using an HPX-87H Aminex ion-exclusion column (Bio-Rad, CA) with refractory index detection (glucose) and UV detection at 210 nm (organic acids) as previously described (Becker et al., 2005).

2.4. GC–MS labeling analysis

Mass isotopomer fractions of amino acids from the cell protein were determined by GC–MS as previously described (Wittmann et al., 2004a). For labeling analysis of the glucose monomer contained in the cellular carbohydrates 10 mg of washed cells was hydrolyzed by incubation in 2 mol L^{-1} HCl for 120 min at 100 °C. The hydrolysate was neutralized, filtered and lyophilized as performed for the amino acids. Subsequently derivatization of glucose was performed by 30 min incubation with 50 μL hydroxylamine·HCl (25 mg mL^{-1} in pyridine) at 80 °C followed by further derivatization into the trimethylsilyl derivate as described previously (Kiefer et al., 2004). The relative fractions of the different mass isotopomers were quantified in triplicate in selective ion monitoring mode.

2.5. Fluxome calculation

For flux calculation all mass isotopomer distributions were corrected for the natural abundance of all stable isotopes and unlabeled biomass from the inoculum. The correction of the latter was carried out by considering that the cells finally harvested for the flux calculation contained a fraction of non-labeled protein which originated from the non-labeled inoculum. Its contribution was quantified by differential analysis of the cell concentration at the beginning and the end of the flux experiment. The corrected mass isotopomer distributions together with directly measured fluxes and metabolite balances around intracellular pools were used to calculate the free fluxes in the network by using an isotopomer model as described previously (Wittmann, 2007; Wittmann and Heinzle, 2002; Wittmann et al., 2004b). The metabolic network of *E. coli* was adapted from literature (Fischer and Sauer, 2003; Peng et al., 2004; Zhao et al., 2004). The precursor requirement for anabolism was calculated from the cellular composition of *E. coli,* which was taken from previous measurement of protein, lipid, DNA, RNA, carbohydrate content (Weber et al., 2002) and the composition of each fraction (Ingraham et al., 1983). Additionally, for producing cells, the precursor demand for hFGF-2 formation was taken into account, which was based on the measured cellular content of the recombinant protein and its amino acid sequence.

Table 1
Impact of plasmid maintenance and heterologous synthesis of hFGF-2 on specific growth rate (μ) of *E. coli* TG1, *E. coli* TG1 pCYTEXP1 and *E. coli* TG1 pλFGFB at 30 °C (no hFGF-2 synthesis) and at 42 °C (induced hFGF-2 synthesis)

	$\mu_{30°C}$ (h^{-1})	$\mu_{42°C}$ (h^{-1})
E. coli TG1	0.57 ± 0.01	0.75 ± 0.07
E. coli TG1 pCYTEXP1	0.56 ± 0.01	0.43 ± 0.01
E. coli TG1 pλFGFB	0.56 ± 0.01	0.29 ± 0.01

Data are mean values from three cultivations with corresponding deviation.

2.6. Metabolome analysis

Extraction of intracellular metabolites was carried out by spraying 5 mL cell suspension into a vacuum-sealed test tube containing 1 mL perchloric acid (70%, −25 °C). After a freeze–thaw cycle between 0 and −25 °C, the pH of the extract was adjusted on ice to pH 7.2–7.4 using KOH, followed by centrifugation (15 s, 12000 × *g*, centrifuge 5417, Eppendorf, Hamburg, Germany) and filtration (0.45 μm, Millipore, Schwalbach, Germany). For measurement of 3-phosphoglycerate (3PG) the pH of the sample was adjusted to 3.5–4.0 with KOH. AMP, ADP, and ATP were analyzed by ion-pair HPLC (Ryll and Wagner, 1991). All other metabolites were quantified by enzymatic analysis (Bergmeyer et al., 1974). Since pyruvate was also excreted into the medium, its intracellular concentration was determined by subtracting the extracellular from the total pyruvate concentration. The concentrations given are related to the cell volume of *E. coli* which is 2.15 mL g^{-1} (Pramanik and Keasling, 1997).

3. Results

3.1. Growth and hFGF-2 production

Both recombinant strains exhibited a significantly lower specific growth rate at 42 °C as compared to 30 °C, whereby the growth inhibition was most pronounced for the hFGF-2 producing strain (Table 1). As found for the specific growth rate also the biomass yield was significantly reduced at 42 °C, whereby the lowest value resulted for the hFGF-2 producing strain (Table 2). The level of by-products was strongly increased at 42 °C, whereby acetate was the dominating compound (Table 2). Concerning hFGF-2 production, the intracellular level of the recombinant protein increased rapidly at 42 °C and reached a cellular content of about 75 mg (g cell dry mass)$^{-1}$, whereby highest production already occurred during the first hour (Fig. 1).

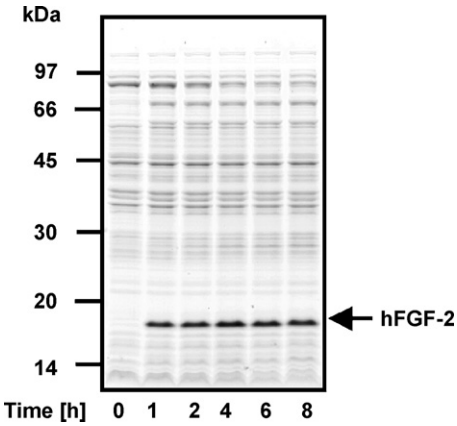

Fig. 1. Specific hFGF-2 concentration during production in batch culture of *E. coli* TG1:pλFGFB. The production was induced by temperature shift from 30 to 42 °C.

3.2. Fluxes at the G6P node towards glycolysis, PPP and EDP

Recombinant protein production was characterized by a flux redirection from the PPP to glycolysis (Fig. 2, Table 4). The flux channeled into the PPP during production was just enough to meet the anabolic requirement for P5P and E4P. As consequence no carbon was redirected back into the glycolysis, so that the PPP did not function as a cycle, which was different from growth. Together with the decreased flux from glycolytic precursors towards anabolism, this resulted in a significantly increased flux through the glycolysis. During growth as well as during production, the EDP was found almost non-active.

3.3. Fluxes at the pyruvate node—connection between glycolysis, TCA cycle and overflow metabolism

The onset of production caused a massive alteration of carbon fluxes at the pyruvate node. This involved a redirection of fluxes towards anabolism, through PEP carboxylase and also through pyruvate dehydrogenase towards the TCA cycle (Fig. 2). In contrast overflow metabolism was strongly enhanced. The formation flux of acetate, pyruvate and lactate was about five-fold higher during production than during growth (Table 4). The

Table 2
Specific growth rate (μ) and yield coefficients (Y) for biomass and by-products of *E. coli* TG1 pCYTEXP1 and *E. coli* TG1 pλFGFB grown at 30 °C (growth conditions) and at 42 °C (production conditions) as mean values from two replicates with corresponding deviation

	pCYTEXP1 (30 °C)	pCYTEXP1 (42 °C)	pλFGFB (30 °C)	pλFGFB (42 °C)
μ (h^{-1})	0.54 ± 0.01	0.45 ± 0.02	0.55 ± 0.01	0.32 ± 0.02
$Y_{Biomass/glucose}$ (mg $mmol^{-1}$)	87 ± 2	68 ± 6	87 ± 1	48 ± 6
$Y_{Acetate/glucose}$ (mmol $mol)^{-1}$	167 ± 15	599 ± 17	177 ± 7	815 ± 13
$Y_{Pyruvate/glucose}$ (mmol $mol)^{-1}$	10 ± 7	4 ± 1	6 ± 1	48 ± 6
$Y_{Lactate/glucose}$ (mmol $mol)^{-1}$	3 ± 0	14 ± 1	6 ± 1	23 ± 7
$Y_{Succinate/glucose}$ (mmol $mol)^{-1}$	4 ± 0	13 ± 1	6 ± 1	2 ± 0

Cells were grown on [1-^{13}C] glucose for metabolic flux analysis.

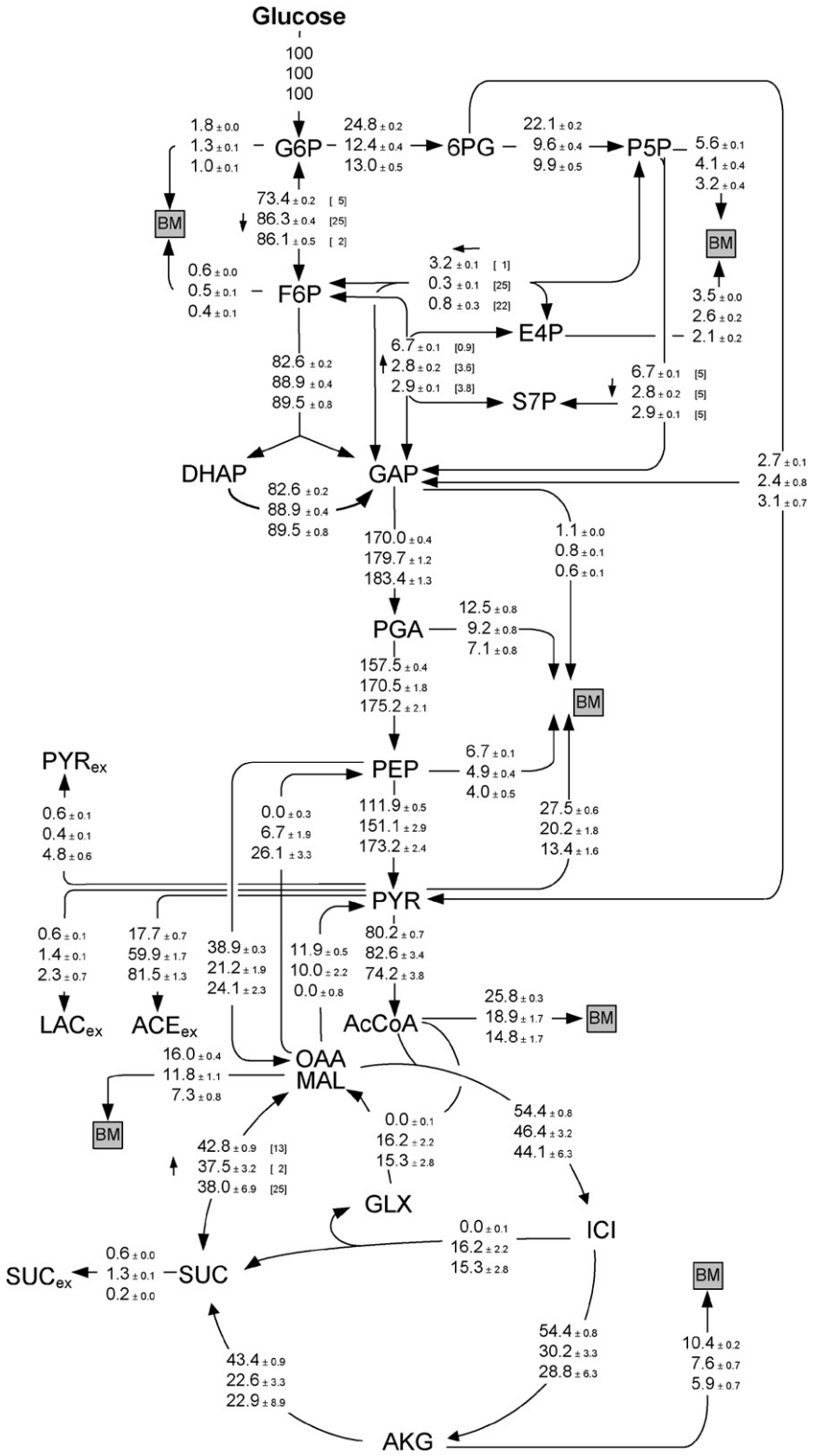

Fig. 2. Metabolic flux analysis of different *E. coli* strains during production of the recombinant growth factor hFGF-2. *In vivo* carbon fluxes in the central metabolism of *E. coli* TG1:pλFGFB under growth conditions at 30 °C (upper), and of *E. coli* TG1:pCYTEXP1 (middle) and *E. coli* TG1:pλFGFB (lower) under production conditions at 42 °C. All fluxes are expressed as a molar percentage of the mean specific glucose uptake rate, which is set to 100%. The mean specific glucose uptake rate was 6.3 mmol g^{-1} h^{-1} for *E. coli* TG1:pλFGFB at 30 °C, 6.7 mmol g^{-1} h^{-1} for *E. coli* TG1:pCYTEXP1 at 42 °C, and 6.8 mmol g^{-1} h^{-1} for *E. coli* TG1:pλFGFB at 42 °C. For reversible reactions the direction of the net flux is indicated by an arrow aside the corresponding box and the flux reversibility is given in brackets below the corresponding net flux value. The fluxes of control and production strain at 30 °C were highly similar. The values given in the figure reflect those of the production strain, but can be taken as representative also for the control strain (data not shown). Concerning the determined fluxes, excellent agreement between experimentally determined and calculated mass isotopomer ratios was achieved for each case (Table 3). For all examined strains, identical flux distributions were obtained with multiple randomized initialization for the free flux parameters, suggesting that global minima were identified in each case.

Table 3
Relative mass isotopomer fractions of amino acids from the cell protein and of glucose from cell carbohydrate from tracer studies of recombinant *E. coli* strains TG1:pCYTEXP1 and TG1:pλFGFB cultivated on 99% [1-^{13}C] glucose at 30 °C (growth conditions) and 42 °C (production conditions)

Analyte		TG1:pλFGFB (30 °C, growth)		TG1:pCYTEXP1 (42 °C, production)		TG1:pλFGFB (42 °C, production)	
		exp	calc	exp	calc	exp	calc
Ala (*m/z* 260)	M_0	0.429	0.426	0.395	0.397	0.395	0.402
	M_1	0.413	0.419	0.437	0.431	0.435	0.426
	M_2	0.118	0.118	0.125	0.130	0.126	0.131
Val (*m/z* 288)	M_0	0.245	0.246	0.215	0.212	0.225	0.220
	M_1	0.415	0.415	0.407	0.405	0.406	0.405
	M_2	0.241	0.242	0.270	0.266	0.263	0.260
Thr (*m/z* 404)	M_0	0.260	0.263	0.224	0.225	0.231	0.235
	M_1	0.384	0.385	0.371	0.374	0.374	0.376
	M_2	0.231	0.229	0.255	0.252	0.251	0.247
Asp (*m/z* 418)	M_0	0.263	0.263	0.226	0.225	0.236	0.234
	M_1	0.383	0.384	0.370	0.373	0.372	0.375
	M_2	0.230	0.229	0.253	0.252	0.247	0.247
Lys (*m/z* 431)	M_0	0.165	0.158	0.126	0.125	0.123	0.131
	M_1	0.332	0.336	0.286	0.306	0.293	0.311
	M_2	0.289	0.289	0.309	0.302	0.302	0.300
	M_3	0.142	0.145	0.171	0.171	0.167	0.167
Ser (*m/z* 390)	M_0	0.384	0.384	0.355	0.363	0.355	0.369
	M_1	0.405	0.405	0.421	0.416	0.419	0.409
	M_2	0.154	0.154	0.161	0.160	0.163	0.161
Phe (*m/z* 336)	M_0	0.185	0.186	0.169	0.169	0.171	0.176
	M_1	0.371	0.371	0.361	0.362	0.363	0.362
	M_2	0.286	0.282	0.297	0.291	0.295	0.285
	M_3	0.116	0.116	0.124	0.125	0.122	0.125
Tyr (*m/z* 466)	M_0	0.162	0.160	0.146	0.146	0.156	0.151
	M_1	0.339	0.338	0.330	0.329	0.330	0.329
	M_2	0.288	0.287	0.299	0.293	0.293	0.288
	M_3	0.140	0.142	0.148	0.151	0.144	0.149
Gly (*m/z* 246)	M_0	0.748	0.750	0.743	0.745	0.724	0.728
	M_1	0.177	0.178	0.181	0.182	0.194	0.196
Glc (*m/z* 612)	M_0	0.029	0.029	0.023	0.023	0.022	0.022
	M_1	0.445	0.456	0.449	0.446	0.436	0.445
	M_2	0.265	0.260	0.267	0.266	0.269	0.266
	M_3	0.159	0.164	0.165	0.170	0.172	0.170
Glu (*m/z* 432)	M_0	0.177	0.174	0.142	0.138	0.148	0.144
	M_1	0.347	0.349	0.319	0.322	0.325	0.326
	M_2	0.279	0.281	0.299	0.300	0.295	0.297
	M_3	0.135	0.134	0.160	0.160	0.155	0.156
Arg (*m/z* 442)	M_0	0.152	0.153	0.135	0.127	0.136	0.131
	M_1	0.329	0.328	0.302	0.307	0.306	0.310
	M_2	0.290	0.289	0.299	0.301	0.297	0.299
	M_3	0.151	0.150	0.168	0.170	0.166	0.167

The data given are experimental values (exp) from GC–MS analysis of the amino acids as *t*-butyl-dimethylsilyl derivates and of glucose as trimethylsilyl derivate and calculated values (calc) predicted by the solution of the mathematical model corresponding to the optimized set of fluxes. M_0 denotes the relative amount of non-labeled mass isotopomer fraction, M_1 the relative amount of the single labeled mass isotopomer fraction, and corresponding terms stand for higher labeling.

two conditions, growth and production, yielded a completely different picture concerning the relative contribution PEP carboxylase and glyoxylate shunt to anaplerosis. During growth the route via PEP carboxylase was the sole anaplerotic pathway. Here, the glyoxylate shunt was not active. During production, the flux through PEP carboxylase was reduced almost two-fold. This was compensated by the activation of the glyoxylate shunt, which then even displayed the dominating anaplerotic pathway. Additionally the flux through PEP carboxykinase, catalyzing the conversion of oxaloacetate towards PEP, was activated. As a result the anaplerotic net flux from the PEP pool into the TCA cycle diminished. Alternatively to the *pox* pathway for acetate formation (as indicated in Fig. 2), acetate formation in *E. coli* can also occur via the *pta-ack* reactions with acetyl-CoA as pre-

Table 4
Flux partitioning at key branch points in central metabolism of recombinant *E. coli* TG1:pλFGFB cultivated at 30 °C (growth conditions) and 42 °C (production conditions)

Metabolic pathways	Flux partitioning during growth (%)	Flux partitioning during production (%)
Flux partitioning at the G6P node		
Glycolysis	74	87
PPP	23	10
EDP	3	3
Flux partitioning at the PEP/PYR node		
Anabolism	24	10
PEP carboxylase	16	0
Overflow metabolism (ACE, LAC, PYR)	11	49
TCA cycle (PYR dehydrogenase)	48	41
Flux partitioning at the ICI node		
TCA cycle (ICI dehydrogenase)	100	65
Glyoxylate shunt (ICI lyase)	0	35

cursor. Implementation of this pathway as alternative route into the metabolic model, however, led to an identical goodness of fit whereby all other reactions in the entire network exhibited identical fluxes. It is therefore not possible on the basis of the labeling data to assign the acetate flux to one of two the possible routes.

3.4. Fluxes at the isocitrate node into the TCA cycle and the glyoxylate shunt

The TCA cycle flux was significantly lower during production as compared to growth (Fig. 2). As example, flux through AKG dehydrogenase and SUC-CoA dehydrogenase was decreased by about 100%. This was to some extent caused by the reduced flux through pyruvate dehydrogenase at the entry in to the TCA cycle. Additionally the activation of the glyoxylate shunt contributed to the decreased TCA cycle flux as indicated by the strong change in the flux partitioning at the isocitrate node (Table 4).

3.5. Flux response of the control strain

The control strain, *E. coli* TG1:pCYTEXP1, incubated a 42 °C revealed a highly changed flux pattern as compared to growth (Fig. 2, middle values). The changes were similar to those observed for the producing strain. However, the magnitude of the redirection of some of the fluxes was less pronounced. Most importantly, the flux through pyruvate dehydrogenase did not decrease upon temperature upshift. As a result, acetate formation was weaker, higher anaplerotic carboxylation was maintained as well as higher anabolic fluxes.

3.6. Influence of biomass requirements

The production of hFGF-2 poses a demand for precursor compounds on the metabolism. For the flux distribution of the production strain shown, it was assumed that the amount of hFGF-2 formed (75 mg g^{-1}) is a fraction of the total protein pool (620 mg g^{-1}). Other imaginable scenarios concerning the anabolic demand were investigated to assess their potential influence on the obtained flux distribution. In detail, it was assumed that (i) the hFGF-2 fraction is formed in addition to the normal cell protein leading to a total protein content of (695 mg g^{-1}) and corrected fractions for the other cell constituents (lipids, DNA, RNA, carbohydrates) or that (ii) hFGF-2 represents 75 mg g^{-1} of the cell, and the other macromolecular fractions (protein, lipids, DNA, RNA, carbohydrates) are corrected such that they represent the remaining 925 mg g^{-1} and exhibit a ratio as in the non-producing cell. None of the cases had a significant influence on the obtained fluxes.

3.7. Intracellular metabolites of glycolysis and PPP

The time course of intracellular metabolite pools of upper and lower glycolysis and from PPP is shown in Fig. 3. Prior to induction, metabolite pools remained constant. The temperature shift then caused an immediate perturbation of the metabolite levels. This involved a highly dynamic change during the initial 30 min and a subsequent stabilization of the pools at the newly reached levels. The concentrations of G6P, F6P and F16BP were decreased up to 70% during production. A drop in concentration was also observed for the pentose phosphate pathway intermediate 6-PG. In contrast, metabolites of lower glycolysis showed a different behavior. Most remarkable was a strong accumulation of the pyruvate pool. The average pyruvate level during production was almost 400% of that observed during growth. The levels of GAP, 3PG and PEP were only slightly affected and, after a transient decrease, almost returned to the values present during growth. DHAP slightly increased.

3.8. Intracellular adenylate nucleotides and energy charge

The intracellular levels of AMP, ADP, and ATP are shown in Fig. 4. Upon induction the ATP level dropped, whereas the low energy adenylates, AMP and ADP, increased. This had strong influence on the overall energy state of the cells as reflected by the adenylate energy charge (AEC). Whereas the AEC remained constant at about 0.85 during normal growth, it immediately dropped with the onset of production and decreased to a value of about 0.60. A similar trend resulted also for the ATP/ADP ratio.

3.9. Mass action ratio of glycolytic enzymes—driving force for pathway flux

The driving force of a reaction can be assessed by its distance from equilibrium (Γ/K_{eq}), i.e. the ratio between the mass action ratio (Γ) and the *in vitro* equilibrium constant (K_{eq}) (Hofmeyr and Cornish-Bowden, 2000). Calculated from the pool size of F6P and FBP, the driving force of the phosphofructokinase reaction, known as key regulator of glycolytic flux in *E. coli* and other organisms was 30% higher for the production phase than for the growth phase (Table 5). To a weaker extent

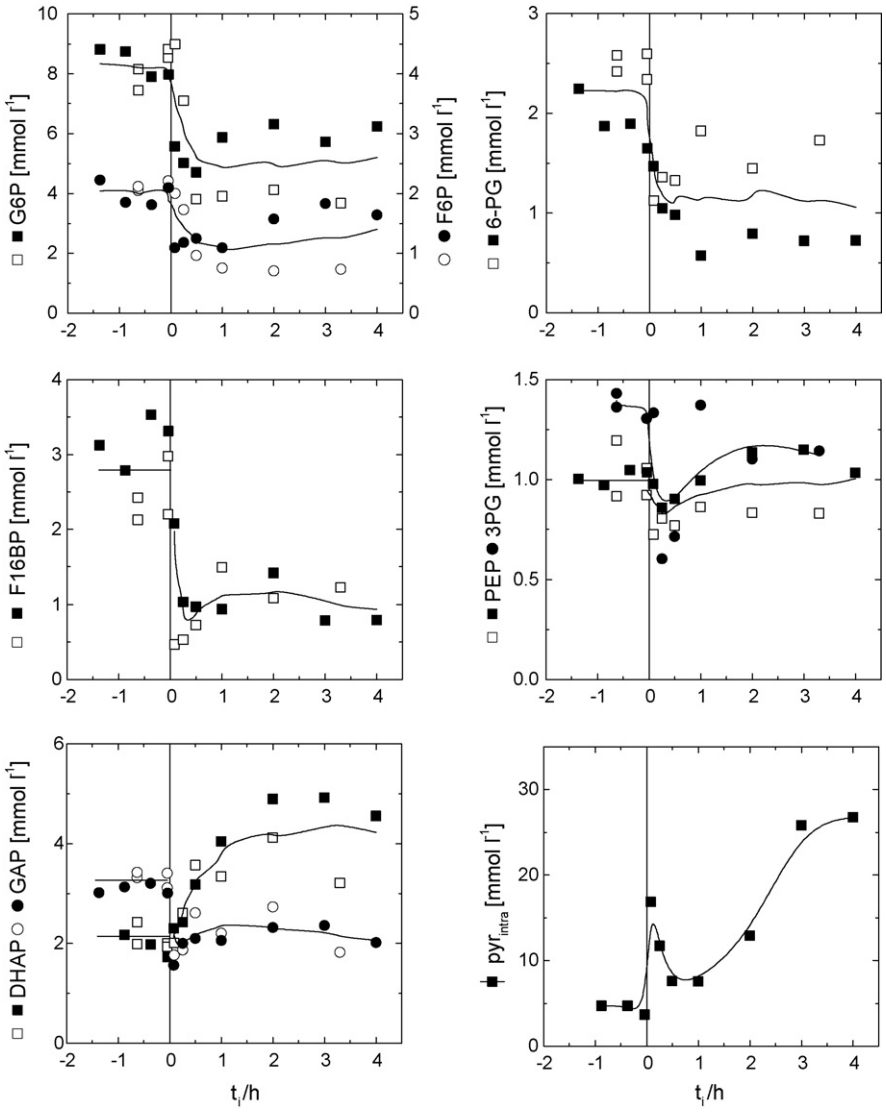

Fig. 3. Intracellular level of metabolites of glycolysis and pentose phosphate pathway in batch culture of *E. coli* TG1:pλFGFB. Cells were grown in batch mode at 30 °C. At a cell density of 3 g L^{-1} the temperature was shifted to 42 °C to induce the synthesis of hFGF-2 (time = 0). Data points from two identical cultivations are shown respectively (trend line serves for better visualization). This study was carried out in a small scale bioreactor, because the metabolome analysis demanded for fast sampling without disturbance of the culture and a sufficient volume for the samples. Upon induction, the cells exhibited a significant reduction of the biomass yield (from 90 to 49 g $mmol^{-1}$), and of the growth rate (from 0.46 to 0. 17 h^{-1}) and a strong enhancement of acetate production (from 85 to 250 mmol mol^{-1}). Thus the overall response of the culture was very similar to that observed for the flux studies.

Table 5
Characteristics of phosphoglucose isomerase (PGI) and of phosphofructokinase (PFK) in the glycolysis of *E. coli* TG1:pλFGFB during growth at 30 °C and hFGF-2 production at 42 °C

	PGI (G6P → >F6P)	PFK (F6P → F16BP)
K_{eq}	0.3[a]	800[b]
Γ_{growth}	0.25	1.37
$\Gamma_{production}$	0.23	0.96
Γ_{growth}/K_{eq}	0.83	0.017
$\Gamma_{production}/K_{eq}$	0.78	0.012

In vivo mass action ratio (Γ), calculated as average concentration ratio of product to substrate from measured average pool sizes during each phase, *in vitro* equilibrium constant (K_{eq}) and distance from equilibrium (Γ/K_{eq}).

[a] Value from (Wurster and Schneider, 1970).

[b] Value from (Hoffmann and Kopperschlaeger, 1982).

this also resulted for the reaction catalyzed by phosphoglucose isomerase.

4. Discussion

Obviously, the metabolic effects observed are mainly due to the cellular burden imposed by plasmid maintenance and formation of the recombinant product. In contrast to *E. coli* TG1, which showed the typical increase of the specific growth rate with temperature increase (Soini et al., 2005), the recombinant strains revealed a significantly decreased growth rate at the elevated temperature. The control strain, carrying an empty plasmid, showed a metabolic response similar to the production strain, but less pronounced. This is probably due to the strongly enhanced plasmid copy number resulting from the temperature upshift

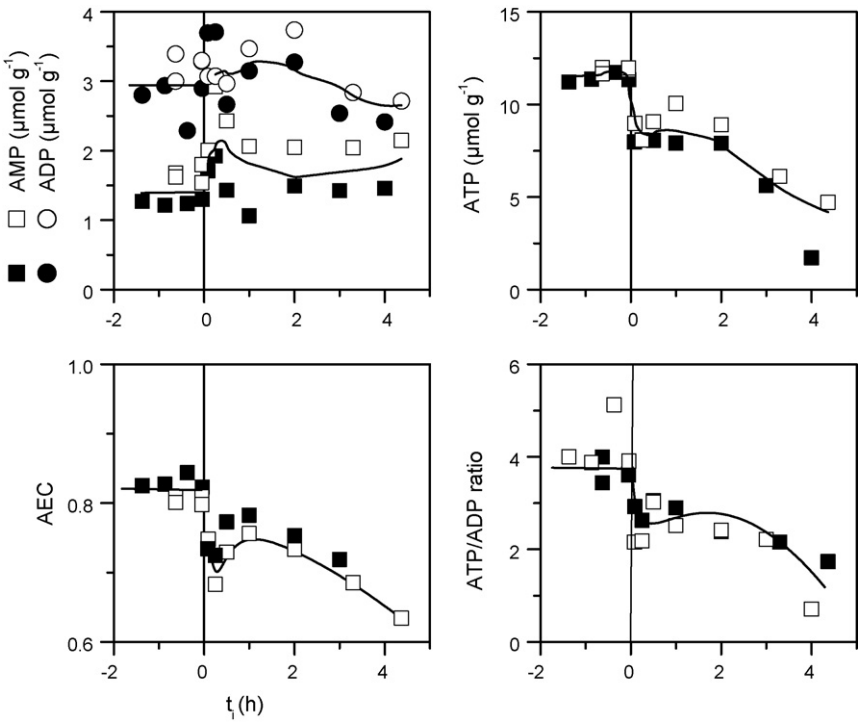

Fig. 4. Intracellular level of adenosine nucleotides and adenylate energy charge (AEC, as defined by (Atkinson, 1968) in *E. coli* TG1:pλFGFB. Cells were grown in batch mode at 30 °C (see also legend of Fig. 3). At a cell density of 3 g L^{-1} the temperature was shifted to 42 °C to induce the synthesis of hFGF-2 (time = 0). Data points from two identical cultivations are shown (trend line serves for better visualization).

leading to increased translation of the plasmid-encoded constitutive proteins and, thus, to stress related metabolic pertubations (Hoffmann and Rinas, 2001).

4.1. Energy status of the cell and activation of glycolytic flux

E. coli TG1:pλFGFB increased the flux through glycolysis as response to the temperature shift and the onset of recombinant protein production. The absolute flux, calculated from the specific glucose uptake rate and the relative glycolytic flux, was about 20% higher during production than during growth. In agreement, the metabolome data, i.e. the increased driving force of phosphofructokinase, indicated an increased glycolytic flux during production. In *E. coli* the glycolytic flux is strongly controlled by the demand for ATP (Koebmann et al., 2002; Zhao et al., 2004). In the given case, a severe drop of the energy level of the cell, i.e. adenylate energy charge and ATP/ADP ratio (Fig. 4), was observed with the onset of production. This energy limitation displays the major signal triggering the activation of the glycolytic flux. It originates from a reduced energy supply on one hand and an increased energy demand on the other hand. As example the overall flux through enzymes supplying reduction equivalents NADH, FADH and NADPH, which all can be utilized for ATP formation in *E. coli*, was reduced from 480% (during growth) to 390% as calculated from the intracellular flux distribution (Fig. 2). The increased ATP demand results from the activation of ATP-consuming reactions such as the induced synthesis of h-FG2 with a demand of 550 µmol ATP (g cells)$^{-1}$ posed in addition to the overall anabolic ATP demand of the cells of 17,985 µmol (g cells)$^{-1}$. Also the formation and activity of stress related proteins such as GroEL and DnaK contributes to an increased ATP demand (Hoffmann and Rinas, 2004).

4.2. Flux redirection at the pyruvate node

The activation of the glycolysis also affected other parts of the metabolic network. *E. coli* revealed a drastic increase of by-product formation upon temperature shift. The extent of the overflow metabolism, especially acetate formation, was significantly higher in the hFGF-2 producing strain, and thus partly caused by the synthesis of the recombinant product itself. We could not resolve the relative contribution of two alternative acetate forming routes, *pox* and the *pta-ack*, so a complete picture of the origin of the enhanced acetate production cannot be given. Different findings of our work and also previous studies, however point at a contribution of the *pox* route to the overflow metabolism. During hFGF-2 production in *E. coli* TG1:pλFGFB LpdA, a component of the pyruvate dehydrogenase complex, partly aggregates which could lead to a limited capacity of the enzyme (Rinas et al., 2007). This is not the case in the control strain, which indeed does not exhibit a reduced flux through pyruvate dehydrogenase. This enzyme often displays a metabolic bottleneck in organisms which exhibit a high glycolytic flux (Frick and Wittmann, 2005). A limited capacity of pyruvate dehydrogenase might also explain the strongly increased intracellular pyruvate pool. The increased availability of pyruvate could then result in an elevated flux through the *pox* pathway. Previous studies of *E. coli* have shown that a flux redirection from pyruvate dehydrogenase to Pox is impor-

tant to overcome metabolic stress during phosphate starvation (Moreau, 2004). A similar mechanism could also result during the metabolic stress linked to recombinant protein production. Future studies with mutants lacking one or both acetate forming pathways seem very interesting to better understand the metabolic changes around the pyruvate node. Moreover these pathways involved display interesting targets to reduce acetate formation, improve recombinant protein production and overcome the energy limitation. During production *E. coli* activated an alternative anaplerotic pathway, the glyoxylate shunt, for replenishment of OAA. The trigger for activation of the glyoxylate pathway could be the elevated acetate level (El-Mansi et al., 2006). The glyoxylate shunt together with acetyl-CoA synthase could be recruited to recycle carbon from the acetate formed back into the TCA cycle. Assuming, that indeed pyruvate oxidase contributes to the acetate formation, the concerted action of these enzymes could create a metabolic by-pass from pyruvate into the TCA cycle around the limiting pyruvate dehydrogenase. Such a metabolic by-pass has been proposed for pyruvate dehydrogenase-deficient *E. coli* (Li et al., 2006), in which indeed *pox* is up-regulated (Abdel-Hamid et al., 2001). Moreover, increased expression of acetyl CoA-synthase (Veit et al., 2007) and the glyoxylate pathway (Phue et al., 2005) correlates with reduced acetate formation. One might consider an amplification of the enzymes probably involved in acetate recycling, such as acetyl-CoA synthase and the enzymes of the glyoxylate shunt, to activate the metabolic by-pass around pyruvate dehydrogenase.

Acknowledgements

Eriola Betiku gratefully acknowledges financial support by the Deutscher Akademischer Austauschdienst (DAAD). Jens Krömer acknowledges financial support of the BASF AG (Ludwigshafen, Germany).

References

Abdel-Hamid, A.M., Attwood, M.M., Guest, J.R., 2001. Pyruvate oxidase contributes to the aerobic growth efficiency of *Escherichia coli*. Microbiology 147, 1483–1498.

Atkinson, D.E., 1968. The energy charge of the adenylate pool as a regulatory parameter. Interaction with feedback modifiers. Biochemistry 7, 4030–4040.

Balbas, P., 2001. Understanding the art of producing protein and nonprotein molecules in *Escherichia coli*. Mol. Biotechnol. 19, 251–267.

Becker, J., Heinzle, E., Klopprogge, C., Zelder, O., Wittmann, C., 2005. Amplified Expression of Fructose 1,6-bisphosphatase in *Corynebacterium glutamicum* increases in vivo flux through the pentose phosphate pathway and lysine production on different carbon sources. Appl. Environ. Microbiol. 71, 8587–8596.

Bergmeyer, H.U., Bergmeyer, J., Grass, M., 1974. Methods of Enzymatic Analysis. Verlag Chemie.

Carter, P., Bedouelle, H., Winter, G., 1985. Improved oligonucleotide site-directed mutagenesis using M13 vectors. Nucleic Acids Res. 13, 4431–4443.

De Anda, R., Lara, A.R., Hernandez, V., Hernandez-Montalvo, V., Gosset, G., Bolivar, F., Ramirez, O.T., 2006. Replacement of the glucose phosphotransferase transport system by galactose permease reduces acetate accumulation and improves process performance of *Escherichia coli* for recombinant protein production without impairment of growth rate. Metab. Eng. 8, 281–290.

El-Mansi, M., Cozzone, A.J., Shiloach, J., Eikmanns, B.J., 2006. Control of carbon flux through enzymes of central and intermediary metabolism during growth of *Escherichia coli* on acetate. Curr. Opin. Microbiol. 9, 173–179.

Fischer, E., Sauer, U., 2003. Metabolic flux profiling of *Escherichia coli* mutants in central carbon metabolism using GC–MS. Eur. J. Biochem. 270, 880–891.

Hoffmann, E., Kopperschlaeger, G., 1982. Phosphofructokinase from yeast. Methods Enzymol. 90, 49–60.

Hoffmann, F., Rinas, U., 2001. Plasmid amplification in *Escherichia coli* after temperature upshift is impaired by induction of recombinant protein synthesis. Biotechnol. Lett. 23, 1819–1825.

Hoffmann, F., Rinas, U., 2004. Stress induced by recombinant protein production in *Escherichia coli*. Adv. Biochem. Eng. Biotechnol. 89, 73–92.

Hofmeyr, J.S., Cornish-Bowden, A., 2000. Regulating the cellular economy of supply and demand. FEBS Lett. 476, 47–51.

Ingraham, J.L., Maaloe, O., Neidhardt, F.C., 1983. Growth of the Bacterial Cell. Sinauer Associates, Inc.

Kiefer, P., Heinzle, E., Zelder, O., Wittmann, C., 2004. Comparative metabolic flux analysis of lysine-producing *Corynebacterium glutamicum* cultured on glucose or fructose. Appl. Environ. Microbiol. 70, 229–239.

Kim, J.Y., Cha, H.J., 2003. Down-regulation of acetate pathway through antisense strategy in *Escherichia coli*: improved foreign protein production. Biotechnol. Bioeng. 83, 841–853.

Koebmann, B.J., Westerhoff, H.V., Snoep, J.L., Nilsson, D., Jensen, P.R., 2002. The glycolytic flux in *Escherichia coli* is controlled by the demand for ATP. J. Bacteriol. 184, 3909–3916.

Korz, D.J., Rinas, U., Hellmuth, K., Sanders, E.A., Deckwer, W.D., 1995. Simple fed-batch technique for high cell density cultivation of *Escherichia coli*. J. Biotechnol. 39, 59–65.

Li, M., Ho, P.Y., Yao, S., Shimizu, K., 2006. Effect of lpdA gene knockout on the metabolism in *Escherichia coli* based on enzyme activities, intracellular metabolite concentrations and metabolic flux analysis by ^{13}C-labeling experiments. J. Biotechnol. 122, 254–266.

Moreau, P.L., 2004. Diversion of the metabolic flux from pyruvate dehydrogenase to pyruvate oxidase decreases oxidative stress during glucose metabolism in nongrowing *Escherichia coli* cells incubated under aerobic, phosphate starvation conditions. J. Bacteriol. 186, 7364–7368.

Peng, L., Arauzo-Bravo, M.J., Shimizu, K., 2004. Metabolic flux analysis for a ppc mutant *Escherichia coli* based on ^{13}C-labelling experiments together with enzyme activity assays and intracellular metabolite measurements. FEMS Microbiol. Lett. 235, 17–23.

Phue, J.N., Noronha, S.B., Hattacharyya, R., Wolfe, A.J., Shiloach, J., 2005. Glucose metabolism at high density growth of *E. coli* B and *E. coli* K: differences in metabolic pathways are responsible for efficient glucose utilization in *E. coli* B as determined by microarrays and Northern blot analyses. Biotechnol. Bioeng. 90, 805–820.

Picon, A., Teixeira de Mattos, M.J., Postma, P.W., 2005. Reducing the glucose uptake rate in *Escherichia coli* affects growth rate but not protein production. Biotechnol. Bioeng. 90, 191–200.

Pramanik, J., Keasling, J.D., 1997. Stoichiometric model of *Escherichia coli* metabolism: Incorporation of growth-rate dependent biomass composition and mechanistic energy requirements. Biotechnol. Bioeng. 56, 398–421.

Rinas, U., Hoffmann, F., Betiku, E., Estape, D., Marten, S., 2007. Inclusion body anatomy and functioning of chaperone-mediated in vivo inclusion body disassembly during high-level recombinant protein production in *Escherichia coli*. J. Biotechnol. 127, 244–257.

Ryll, T., Wagner, R., 1991. Improved ion-pair high-performance liquid chromatographic method for the quantification of a wide variety of nucleotides and sugar-nucleotides in animal cells. J. Chromatogr. 570, 77–88.

Seeger, A., Schneppe, B., McGarthy, J.E.G., Deckwer, W.D., Rinas, U., 1995. Comparison of temperature- and isopropyl-beta-D-thiogalacto-pyranoside-induced synthesis of basic fibroblast growth factor in high-cell-density cultures of recombinant *Escherichia coli*. Enzyme Microb. Technol. 17, 947–953.

Soini, J., Falschlehner, C., Mayer, C., Bohm, D., Weinel, S., Panula, J., Vasala, A., Neubauer, P., 2005. Transient increase of ATP as a response to temperature up-shift in *Escherichia coli*. Microb. Cell Fact. 4, 9.

Sorensen, H.P., Mortensen, K.K., 2005. Advanced genetic strategies for recombinant protein expression in *Escherichia coli*. J. Biotechnol. 115, 113–128.

Veit, A., Polen, T., Wendisch, V.F., 2007. Global gene expression analysis of glucose overflow metabolism in *Escherichia coli* and reduction of aerobic acetate formation. Appl. Microbiol. Biotechnol. 74, 406–421.

Weber, J., Hoffmann, F., Rinas, U., 2002. Metabolic adaptation of *Escherichia coli* during temperature-induced recombinant protein production. 2. Redirection of metabolic fluxes. Biotechnol. Bioeng. 80, 320–330.

Wegrzyn, G., Wegrzyn, A., 2002. Stress responses and replication of plasmids in bacterial cells. Microb. Cell Fact. 1, 2.

Wittmann, C., 2007. Fluxome analysis using GC-MS. Microb. Cell Fact. 6, 6.

Wittmann, C., Heinzle, E., 2002. Genealogy profiling through strain improvement by using metabolic network analysis: metabolic flux genealogy of several generations of lysine-producing corynebacteria. Appl. Environ. Microbiol. 68, 5843–5859.

Wittmann, C., Kiefer, P., Zelder, O., 2004a. Metabolic fluxes in *Corynebacterium glutamicum* during lysine production with sucrose as carbon source. Appl. Environ. Microbiol. 70, 7277–7287.

Wittmann, C., Kim, H.M., Heinzle, E., 2004b. Metabolic network analysis of lysine producing *Corynebacterium glutamicum* at a miniaturized scale. Biotechnol. Bioeng. 87, 1–6.

Wurster, B., Schneider, F., 1970. Kinetics of glucosephosphate isomerase (EC 5.3.1.9) from yeast in vitro and its application to flux calculations for the fermentation pathway of anaerobic yeast cells. Hoppe Seylers Z. Physiol. Chem. 351, 961–966.

Zhao, J., Baba, T., Mori, H., Shimizu, K., 2004. Global metabolic response of *Escherichia coli* to gnd or zwf gene-knockout, based on ^{13}C-labeling experiments and the measurement of enzyme activities. Appl. Microbiol. Biotechnol. 64, 91–98.